Title

Production of muconic acid in plants

Authors

Eudes, Aymerick

Berthomieu, Roland

Hao, Zhangying

et al.

Publication Date

2018-03-01

DOI

10.1016/j.ymben.2018.02.002

Peer reviewed

Metabolic Engineering 46 (2018) 13–19

Contents lists available at ScienceDirect

Metabolic Engineering

journal homepage: www.elsevier.com/locate/meteng

Production of muconic acid in plants

Aymerick Eudes[a,b,*], Roland Berthomieu[a,c], Zhangying Hao[a,b], Nanxia Zhao[a,d], Veronica Teixeira Benites[a,e], Edward E.K. Baidoo[a,e], Dominique Loqué[a,b,f,g,*]

[a] Joint BioEnergy Institute, EmeryStation East, 5885 Hollis St, 4th Floor, Emeryville, CA 94608, USA
[b] Environmental Genomics and Systems Biology Division, Lawrence Berkeley National Laboratory, 1 Cyclotron Road, Berkeley, CA 94720, USA
[c] Ecole Polytechnique, Université Paris-Saclay, Palaiseau 91120, France
[d] Department of Bioengineering, Department of Chemical & Biomolecular Engineering, University of California, Berkeley, CA 94720, USA
[e] Biological Systems and Engineering Division, Lawrence Berkeley National Laboratory, 1 Cyclotron Road, Berkeley, CA 94720, USA
[f] Department of Plant and Microbial Biology, University of California, Berkeley, CA 94720, USA
[g] Université Lyon 1, INSA de Lyon, CNRS, UMR5240, Microbiologie, Adaptation et Pathogénie, 10 rue Raphaël Dubois, F-69622, Villeurbanne, France

ARTICLE INFO

Keywords:
Muconic acid
Salicylic acid
Catechol
Shikimate
Plastid
Arabidopsis

ABSTRACT

Muconic acid (MA) is a dicarboxylic acid used for the production of industrially relevant chemicals such as adipic acid, terephthalic acid, and caprolactam. Because the synthesis of these polymer precursors generates toxic intermediates by utilizing petroleum-derived chemicals and corrosive catalysts, the development of alternative strategies for the bio-based production of MA has garnered significant interest. Plants produce organic carbon skeletons by harvesting carbon dioxide and energy from the sun, and therefore represent advantageous hosts for engineered metabolic pathways towards the manufacturing of chemicals. In this work, we engineered Arabidopsis to demonstrate that plants can serve as green factories for the bio-manufacturing of MA. In particular, dual expression of plastid-targeted bacterial salicylate hydroxylase (NahG) and catechol 1,2-dioxygenase (CatA) resulted in the conversion of the endogenous salicylic acid (SA) pool into MA via catechol. Sequential increase of SA derived from the shikimate pathway was achieved by expressing plastid-targeted versions of bacterial salicylate synthase (Irp9) and feedback-resistant 3-deoxy-D-arabino-heptulosonate synthase (AroG). Introducing this SA over-producing strategy into engineered plants that co-express NahG and CatA resulted in a 50-fold increase in MA titers. Considering that MA was easily recovered from senesced plant biomass after harvest, we envision the phytoproduction of MA as a beneficial option to add value to bioenergy crops.

1. Introduction

Muconic acid (MA) is a platform chemical that serves as a precursor for the synthesis of products such as adipic acid, terephthalic acid, and caprolactam which are widely used in the nylon and thermoplastic polymer industries. Current processes for the manufacturing of MA or its derivatives mainly rely on non-renewable petroleum-based chemicals. Such processes are not sustainable and eco-friendly since they require a high energy input and yield large quantities of toxic by-products (Xie et al., 2014).

As an alternative, the biological production of MA using engineered microorganisms and inexpensive carbohydrate feedstocks has received increasing attention over the past 20 years (Xie et al., 2014). Most of the established biological routes consist in the production catechol and its subsequent conversion into MA by ring-cleaving catechol 1,2-dioxygenase (Vaillancourt et al., 2006). All these routes exploit the intrinsic shikimate pathway for the biosynthesis of catechol precursors such as protocatechuate, anthranilate, salicylic acid (SA), and 2,3-dihydroxybenzoic acid (Kruyer and Peralta-Yahya, 2017). Recently, MA biosynthetic pathways have been implemented in various microbial strains capable of growing in the presence of aromatics derived from lignocellulosic biomass. These include engineered strains of *Escherichia coli* (Sonoki et al., 2014; Wu et al., 2017), *Amycolatopsis* sp. (Barton et al., 2017), *Pseudomonas* sp. (Vardon et al., 2015; Johnson et al., 2016, 2017; Sonoki et al., 2017), and *Sphingobium* sp. (Sonoki et al., 2017).

In addition to microbial synthesis, the metabolic engineering of photosynthetic organisms like plants also provides a sustainable approach for the production of valuable metabolites and materials (Börnke and Broer, 2010; Farré et al., 2014). These chemicals, when produced in engineered bioenergy and oilseed crops, represent value-added renewable co-products on top of the lignocellulose and seed oil

Abbreviations: DAHP, 3-deoxy-D-arabino-heptulosonate; MA, muconic acid; SA, salicylic acid

* Corresponding authors at: Environmental Genomics and Systems Biology Division, Lawrence Berkeley National Laboratory, 1 Cyclotron Road, Berkeley, CA 94720, USA.
E-mail addresses: ageudes@lbl.gov (A. Eudes), dloque@berkeley.edu (D. Loqué).

https://doi.org/10.1016/j.ymben.2018.02.002
Received 1 October 2017; Received in revised form 6 January 2018; Accepted 13 February 2018
Available online 21 February 2018

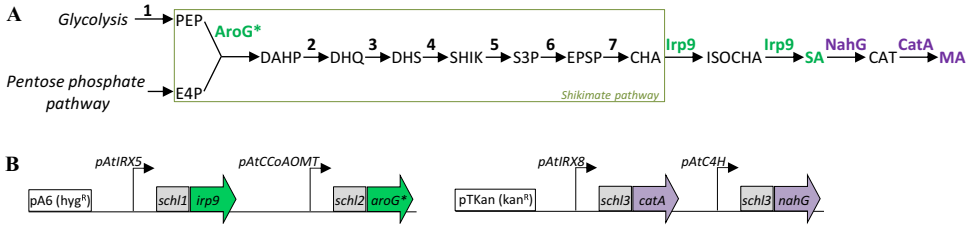

Fig. 1. Strategy used for the production of muconic acid in plants. (A) De novo biosynthetic pathway for muconic acid synthesis. Bacterial enzymes AroG*, Irp9, NahG, and CatA were expressed in Arabidopsis for the production of muconic acid from salicylic acid derived from the shikimate pathway. Abbreviations are: CAT, catechol; CHA, chorismate; DAHP, 3-deoxy-D-arabino-heptulosonate; DHQ, dehydroquinate; DHS, dehydroshikimate; E4P, erythrose 4-phosphate; EPSP, 5-enolpyruvoylshikimate 3-phosphate; F6P, fructose 6-phosphate; G3P, glyceraldehyde 3-phosphate; ISOCHA, isochorismate; MA, muconic acid; PEP, phosphoenolpyruvate; PYR, pyruvate; S3P, shikimate 3-phosphate; SA, salicylic acid; SHIK, shikimate. The enzymes are as follows: 1, enolase; AroG*, feedback-resistant DAHP synthase (L175Q); 2, DHQ synthase; 3, DHQ dehydratase; 4, shikimate dehydrogenase; 5, shikimate kinase; 6, EPSP synthase; 7, chorismate synthase; Irp9, bifunctional ISOCHA synthase / ISOCHA pyruvate lyase; NahG, salicylate hydroxylase; CatA, catechol 1,2-dioxygenase. (B) Binary vectors used in this study. Boxes labelled "schl" denote plastid transit peptides. pA6 and pTKan denote the two binary vector backbones conferring hygromycin (hyg^R) and kanamycin (kan^R) resistance in plants. Abbreviations are: schl1, plastid transit peptide from Arabidopsis ferredoxin2 (At1g60950); schl2, plastid transit peptide from pea (*Pisum sativum*) ribulose-1,5-bisphosphate carboxylase small subunit (GenBank: AAG45569.1); schl3, plastid transit peptide sunflower (*Helianthus annuus*) ribulose-1,5-bisphosphate carboxylase small subunit (UniProtKB/Swiss-Prot: P08705.1). *pAtIRX5*, *pAtCCoAOMT*, *pAtIRX8*, and *pAtC4H* designate the promoters of Arabidopsis cellulose synthase 4 (At5G44030), caffeoyl coenzyme A O-methyltransferase 1 (At4G34050), galacturonosyltransferase 12 (At5G54690), and cinnamate 4-hydroxylase (At2G30490) genes, respectively.

used to generate energy (Snell et al., 2015). Because plants are autotrophs able to capture solar energy, they represent an attractive chassis for implementing *de novo* metabolic pathways for cost-effective production of important chemicals (Yuan and Grotewold, 2015).

In plants, the shikimate pathway is confined to plastids and provides the precursors for the synthesis of aromatic amino acids and derived metabolites, vitamins K_1 and B_9, and SA (Maeda and Dudareva, 2012). We therefore used Arabidopsis as a model system to investigate a novel bio-based approach for the phytoproduction of MA. In particular, the SA pool derived from chorismate via the shikimate pathway was converted to catechol and MA by dual expression and plastid-targeting of bacterial salicylate hydroxylase (NahG) and catechol 1,2-dioxygenase (CatA) (Fig. 1A). Additional supply of SA to the MA pathway was achieved via the expression of bacterial salicylate synthase Irp9 and feedback-resistant 3-deoxy-D-arabino-heptulosonate (DAHP) synthase (AroG*), which resulted in a ~50-fold increase of MA content. Importantly, MA was recovered from the biomass of senesced mature plants which highlights its stability and suitability for storage when produced in target crops. Therefore, such engineered crops could represent high-potential feedstocks for existing MA microbial production platforms towards sustainable development of bio-based MA.

2. Material and methods

2.1. Plant material and growth conditions

Arabidopsis thaliana (ecotype Columbia, Col-0) seeds were germinated directly on soil. Growing conditions were 150 µmol/m^2/s, 22 °C, 60% humidity and 10 h of light per 24-h day cycle. Selection of T2 and identification of T3 homozygous transgenic plants was made on Murashige and Skoog vitamin medium (PhytoTechnology Laboratories, Shawnee Mission, KS), supplemented with 1% sucrose, 1.5% agar, 50 µg/mL kanamycin and/or 25 µg/mL hygromycin.

2.2. Construction of plasmids and plant transformation

To generate the *pA6-pIRX5*::*schl1-irp9* construct, a gene sequence encoding Irp9 from *Yersinia enterocolitica* (GenBank accession number CAB46570.1) containing the encoding sequence of the plastid transit peptide (schl1) from the Arabidopsis ferredoxin2 (At1g60950) (Xue et al., 2013), and flanked with the Gateway attB1 (5'-end) and attB2 (3'-end) recombination sites was synthesized for expression in Arabidopsis (attB1-*schl1-irp9*-attB2, Supplementary Data S1) (GenScript, Piscatway, NJ). This sequence was cloned into the Gateway pDONR221-P1P2 entry vector by BP recombination (Life technologies, Foster City, CA). An entry clone was LR recombined with the *pA6-pIRX5*::GWR1R2 vector (Vega-Sánchez et al., 2015) to generate the *pA6-pIRX5*::*schl1-irp9* construct.

To generate the *pA6-pIRX5*::*schl1-irp9-pCCoAOMT*::*schl2-aroG* construct (Fig. 1B), the attB1-*schl1-irp9*-attB2 sequence was amplified by PCR to replace the Gateway attB2 recombination site (3'-end) by an attB4 recombination site, and cloned into the Gateway pDONR221-P1P4 entry vector by BP recombination (Life technologies, Foster City, CA) to produce a pDONR221-L1-*schl1-irp9*-L4 construct. A chimeric DNA construct was synthesized (GenScript, Piscatway, NJ): it was flanked by the gateway sequences attB4r (5'-end) and attB3r (3'-end), and contained the *tG7* terminator and a 2.2-Kb sequence corresponding to the *Arabidopsis CCoAOMT1* (*At4g34050*) promoter (*pCCoAOMT*). This attB4r-*tG7-pCCoAOMT*-attB3r construct (Supplementary Data S1) was then subcloned into the Gateway pDONR221-P4rP3r entry vector by BP recombination (Life technologies, Foster City, CA) to produce pDONR221-L4R-*tG7-pCCoAOMT*-L3R. A gene sequence encoding feedback-insensitive AroG (L175Q) from *E. coli* (NCBI Reference Sequence: WP_032246946.1) containing the encoding sequence of the transit peptide (schl2) of the pea (*Pisum sativum*) ribulose-1,5-bisphosphate carboxylase small subunit (GenBank: AAG45569.1) (Tzin et al., 2012), and flanked with the Gateway attB3 (5'-end) and attB2 (3'-end) recombination sites was synthesized for expression in Arabidopsis (attB3-*schl2-aroG*-attB2, Supplementary Data S1) (GenScript, Piscatway, NJ). This sequence was cloned into the Gateway pDONR221-P3P2 entry vector by BP recombination (Life technologies, Foster City, CA) to produce the pDONR221-P3-*schl2-aroG*-P2 construct. A multi-site LR recombination (Life technologies, Foster City, CA, USA) using the pDONR221-L1-*schl1-irp9*-L4, pDONR221-L4R-*tG7-pCCoAOMT*-L3R, and pDONR221-L3-*schl2-aroG*-L2 entry vectors and the *pA6-pIRX5*::GWR1R2 destination vector was performed to generate the *pA6-pIRX5*::*schl1-irp9-pCCoAOMT*::*schl2-aroG* construct.

To generate the *pTkan-pIRX8-schl3-catA-pC4H-schl3-nahG* construct (Fig. 1B), a gene sequence encoding CatA from *Pseudomonas putida* (NCBI Reference Sequence: WP_010954549.1) containing the encoding sequence of the transit peptide (schl3) of the sunflower (*Helianthus annuus*) ribulose-1,5-bisphosphate carboxylase small subunit (UniProtKB/Swiss-Prot: P08705.1) (Lebrun et al., 1992; Eudes et al., 2015), and flanked with the Gateway attB1 (5'-end) and attB4 (3'-end) recombination sites was synthesized for expression in Arabidopsis (attB1-*schl3-catA*-attB4, Supplementary Data S1) (GenScript, Piscatway, NJ). This sequence was cloned into the Gateway pDONR221-P1P4 entry vector by BP recombination (Life technologies, Foster City, CA) to produce the pDONR221-L1-*schl3-catA*-L4 construct. A gene sequence encoding NahG from *Pseudomonas putida* (NCBI Reference Sequence: WP_011475386.1) and flanked with the Gateway attB3 (5'-end) and attB2 (3'-end) recombination sites was synthesized for expression in Arabidopsis (attB3-*nahG*-attB2, Supplementary Data S1) (GenScript, Piscatway, NJ). This sequence was cloned into the Gateway pDONR221-P3P2 entry vector by BP recombination (Life technologies, Foster City, CA) to produce the pDONR221-L3-*nahG*-L2 construct. A multi-site LR recombination (Life technologies, Foster City, CA) using the pDONR221-L1-*schl3-catA*-L4, pDONR221-L4R-*tg7-pC4H*::*schl3*-L3R

(Eudes et al., 2015), and pDONR221-L3-*nahG*-L2 entry vectors and the *pTKan-pIRX8*::GWR1R2 (Yang et al., 2013) destination vector was performed to generate the *pTkan-pIRX8-schl3-catA-pC4H-schl3-nahG* construct. The constructs were introduced into wild-type Arabidopsis plants (ecotype Col0) via *Agrobacterium tumefaciens*-mediated transformation (Bechtold and Pelletier, 1998).

2.3. RNA extraction and qRT-PCR analysis

Total RNA was extracted from stems of 5-week-old wild type and T3 homozygous transgenic lines (pools of three plants per line, ~100 mg) using the Plant RNeasy extraction kit (Qiagen, Valencia, CA), and treated with DNase (Qiagen, Valencia, CA) to remove genomic DNA contamination. First-strand cDNAs were synthesized from 2 µg of total RNA using the SuperScript III First-Strand Synthesis SuperMix (Thermo Fisher Scientific, Waltham, MA) followed by qPCR analysis using SsoAdvanced Universal SYBR Green Supermix (Bio-Rad, Hercules, CA) on a CFX96 Real-Time PCR Detection System (Bio-Rad, Hercules, CA) following the manufacturer's instruction. Oligonucleotide primers (Supplementary Table S1) were tested in annealing temperature gradients and 58 °C was chosen as the annealing temperature. Melting curve analyses were performed after each run to ensure single amplicons were produced. The data were analyzed using the 2^(-ΔΔCt) method (Livak and Schmittgen, 2011).

2.4. Metabolite extraction

SA was extracted from developing stems using 80% (v/v) methanol-water at 70 °C as previously described (Eudes et al., 2015). MA was extracted from stems of mature senesced plants ball-milled with a mixer mill MM 400 (Retsch, Newtown, PA). Ball-milled stem material (50 mg) was mixed with 1 mL of 80% (v/v) methanol-water and mixed (1400 rpm) for 15 min at 70 °C. This extraction step was repeated twice. Extracts were pooled and cleared by centrifugation (5 min, 20,000 × *g*), mixed with 1.5 mL of analytical grade water and filtered using Amicon Ultra centrifugal filters (3000 Da MW cutoff regenerated cellulose membrane; EMD Millipore, Billerica, MA) prior to LC-MS analysis.

Alternatively, MA was released from stems of mature senesced plants (line nahG-catA-1.2 × irp9-aroG 2.2) using dilute alkaline and dilute acid treatments. For dilute alkaline treatments, 10 mg of ball-milled biomass was soaked with 90 µL of either 1.2% or 0.62% (w/v) NaOH and heated at 100 °C or 130 °C for 30 min in an autoclave, respectively. For dilute acid treatment, biomass (10 mg) was soaked with 90 µL of 1.2% (w/v) H_2SO_4 and heated at 120 °C for 30 min in an autoclave. After cooling down and centrifugation, an aliquot of the hydrolyzates was mixed with 4 volumes of 80% (v/v) methanol-water and filtered using Amicon Ultra centrifugal filters prior to LC-MS analysis.

2.5. LC-MS metabolite analysis

SA and catechol were analyzed using liquid chromatography (LC), electrospray ionization (ESI), and time-of-flight (TOF) mass spectrometry (MS) as previously described (Haushalter et al., 2017). LC-ESI-TOF-MS analysis of muconic acid was carried out with a similar method except that the LC gradient elution was conducted as follows: linearly increased from 5% solvent B (0.1% formic acid in methanol) to 60.9% B in 4.3 min, increased from 60.9% B to 97.1% B in 1.3 min, decreased from 97.1% B to 5% B in 0.4 min, and held at 5% B for 2 min. The flow rate was held at 0.42 mL/min for 5.6 min, increased from 0.42 mL/min to 0.65 mL/min in 0.4 min, and held at 0.65 mL/min for 2 min. The total LC run time was 8 min. All metabolites were quantified via calibration curves of standard compounds (Sigma-Aldrich, St Louis, MO) for which the R^2 coefficients were ≥ 0.99. Cis,trans-MA was prepared from cis,cis-MA as previously described (Matthiesen et al., 2016).

3. Results

3.1. Muconic acid (MA) production in plants expressing nahG and catA

The plastidial SA pool derived from the shikimate pathway was used as precursor for the biosynthesis of MA in Arabidopsis stems. To this end, we co-expressed plastid-targeted versions of the salicylate hydroxylase NahG and catechol 1,2-dioxygenase CatA from *Pseudomonas putida* for the sequential conversion of SA into catechol and MA. Although NahG has been shown previously to be functional in plants (Friedrich et al., 1995), the use of CatA for the synthesis of MA in plants has never been described. Since mature senesced Arabidopsis plants mainly consist of stem biomass, we selected two Arabidopsis promoters (*pIRX8* and *pC4H*) which are both strongly active in stem tissues that develop secondary cell walls for synchronized expression of *nahG* and *catA* (Fig. 1B). Specifically, both promoters are known to be active in xylem vessels and interfascicular fibers: *pIRX8* is the promoter of a glycosyltransferase family 8 (GT8) involved in the synthesis of secondary cell wall xylan (Persson et al., 2007), and *pC4H* is the promoter of the cytochrome P450 cinnamate 4-hydroxylase involved in the general phenylpropanoid pathway and lignin biosynthesis (Bell-Lelong et al., 1997). Five independent lines were selected, and expression of *nahG* and *catA* was confirmed by RT-qPCR using mRNA extracted from stems of 5-week-old homozygous plants at the T3 generation (Fig. 2A). For these five lines, the content of MA extracted from stem biomass of senesced plants varied between 8.3 and 13.8 µg/g DW (Fig. 2B), which validates the dual *nahG-catA* expression strategy for the production of MA in plants. Although CatA converts catechol into cis,cis-MA, we detected a mixture of cis,cis-MA and cis,trans-MA in our plant extracts (Supplementary Fig. S1), presumably due to the partial conversion of cis,cis-MA acid during the extraction procedure performed at 70 °C. Therefore, MA titers reported in this work are the sum of cis,cis-MA acid and cis,trans-MA. Moreover, SA content measured in 5-week-old stems from the transgenic lines that co-express *nahG* and *catA* was reduced 5- to 10-fold compared to wild-type plants (Fig. 2C), suggesting that SA could be limiting for MA synthesis in transgenics.

3.2. Enhancement of SA content in stems by expressing bacterial salicylate synthase (Irp9) and feedback-insensitive DAHP synthase (AroG*)

In order to increase the content of SA in Arabidopsis stems, a plastid-targeted version of the salicylate synthase Irp9 from *Yersinia enterocolitica* was expressed using the promoter of the Arabidopsis secondary cell wall cellulose synthase gene *IRX5* (*CESA4*) which is specifically active in stem vascular tissues (Eudes et al., 2012). Expression of *irp9* has previously been shown to be effective to increase SA content without negative growth consequences in poplar (Xue et al., 2013). Seven independent lines were selected and expression of *irp9* was confirmed by RT-qPCR using mRNA extracted from stems of 5-week-old homozygous plants at the T3 generation (Fig. 3A). For six of these seven lines, the content of SA extracted from 5-week-old stems was increased significantly 1.8- to 4.4-fold compared to wild-type plants (Fig. 3B), which validates the important role of Irp9 to increase SA content in Arabidopsis stems. None of these transgenic lines showed any visible growth defects. Next, in order to further increase the carbon flux through the SA biosynthesis pathway in stem, we generated a new set of transgenic lines for co-expression of Irp9 with a mutant feedback-insensitive DAHP synthase (AroG*) from *E. coli*. Expression of plastid-targeted AroG* in Arabidopsis was previously shown to increase the content of metabolites derived from the shikimate pathway such as aromatic amino acids and hydroxycinnamates (Tzin et al., 2012). The promoter *pCCoAOMT* of the caffeoyl-CoA *O*-methyltransferase gene involved in the monolignol pathway and lignin biosynthesis in Arabidopsis was chosen to express *aroG** in stem vascular tissues that produce secondary cell walls (Do et al., 2007). Expression of *irp9* and *aroG** was verified in six independent lines using mRNA extracted from 15-cm

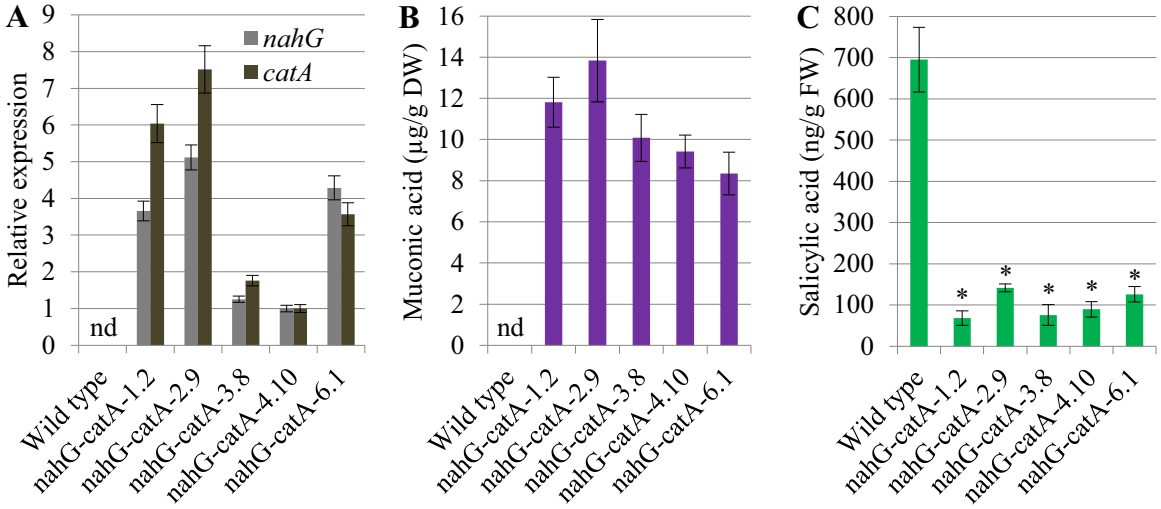

Fig. 2. MA and SA production in plants expressing bacterial NahG and CatA. (A) Detection by qRT-PCR of mRNA expression levels in stems from 5-week-old wild type and *pTkan-pIRX8-schl3-catA-pC4H-schl3-nahG* (nahG-catA) transgenic lines. *ACT2* was used as an internal control. Expression levels of *nahG* and *catA* were normalized to 1 in line nahG-catA-4.10 and were calculated relative to these values in the other lines. Error bars represent the SD from technical duplicates. (B) MA content in mature senesced dried stems of wild type and nahG-catA transgenic lines. Error bars represent the SE from four biological replicates ($n = 4$). (C) SA content in stems of 5-week-old wild type and nahG-catA transgenic lines. Error bars represent the SE from four biological replicates ($n = 4$). Asterisks indicate significant differences from the wild type using the unpaired Student's *t*-test (*$P < 0.005$).

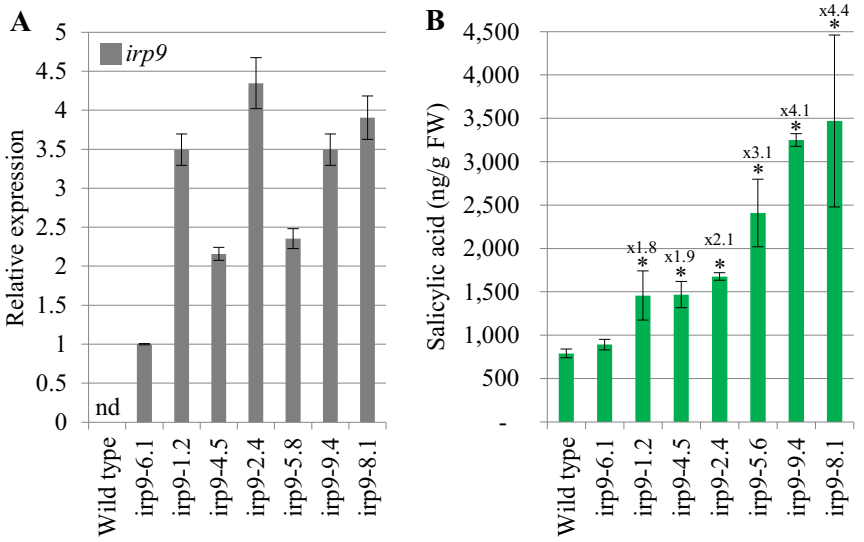

Fig. 3. Overproduction of SA in plants expressing Irp9 and feedback-resistant DAHP synthase (AroG*). (A) Detection by qRT-PCR of mRNA expression levels in stems from 5-week-old wild type and *pA6-pIRX5::schl1-irp9* (irp9) transgenic lines. *ACT2* was used as an internal control. *Irp9* expression level was normalized to 1 in line irp9-6.1 and was calculated relative to this value in the other lines. Error bars represent the SD from technical duplicates. (B) SA content in stems of 5-week-old wild type and irp9 transgenic lines. Error bars represent the SE from four biological replicates ($n = 4$). Asterisks indicate significant differences from the wild type using the unpaired Student's *t*-test (*$P < 0.005$). (C) Detection by qRT-PCR of mRNA expression levels in 15-cm stems from wild type and *pA6-pIRX5::schl1-irp9-pCCoAOMT::schl2-aroG* (irp9-aroG) transgenic lines. *ACT2* was used as an internal control. *Irp9* and *aroG* expression levels were normalized to 1 in line irp9-aroG-6.9 and were calculated relative to these values in the other lines. Error bars represent the SD from technical duplicates. (D) SA content in 15-cm stems of wild type and irp9-aroG transgenic lines. Error bars represent the SE from four biological replicates ($n = 4$). Asterisks indicate significant differences from the wild type using the unpaired Student's *t*-test (*$P < 0.001$).

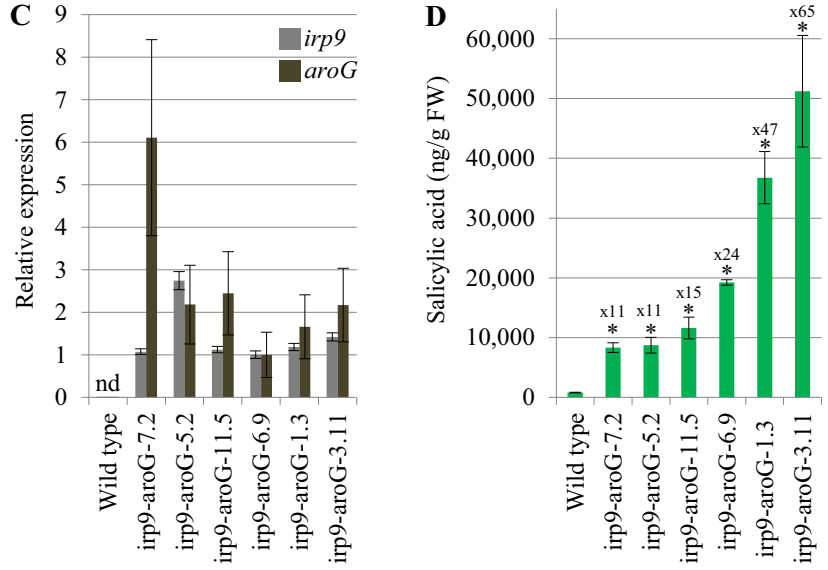

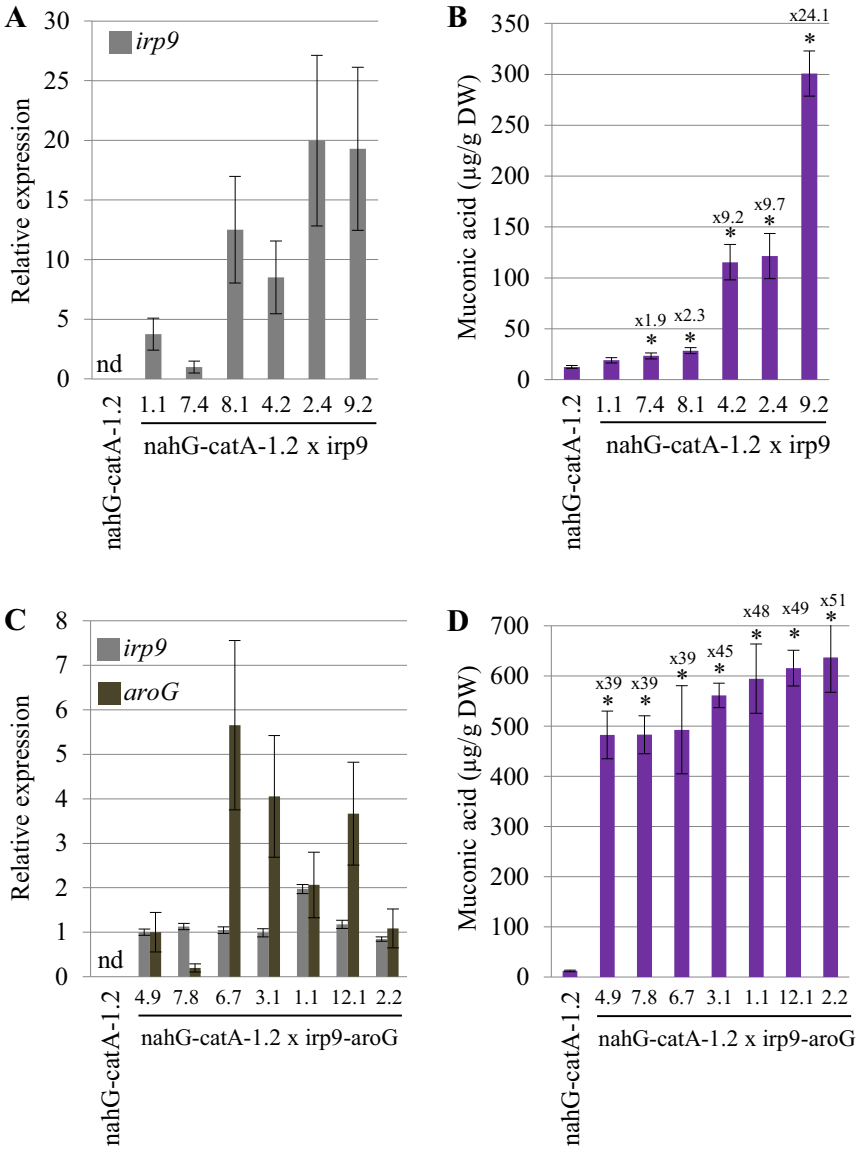

Fig. 4. MA production in plants expressing bacterial NahG, CatA, Irp9 and AroG*. (A) Detection by qRT-PCR of mRNA expression levels in stems from 5-week-old nahG-catA-1.2 and nahG-catA-1.2 × irp9 transgenic lines. *ACT2* was used as an internal control. *Irp9* expression level was normalized to 1 in line nahG-catA-1.2 × irp9 7.4 and was calculated relative to this value in the other lines. Error bars represent the SD from technical duplicates. (B) MA content in mature senesced dried stems of nahG-catA-1.2 and nahG-catA-1.2 × irp9 transgenic lines. Error bars represent the SE from four biological replicates ($n = 4$). Asterisks indicate significant differences from the nahG-catA-1.2 line using the unpaired Student's *t*-test (*$P < 0.05$). (**C**) Detection by qRT-PCR of mRNA expression levels in stems from 5-week-old nahG-catA-1.2 and nahG-catA-1.2 × irp9-aroG transgenic lines. *ACT2* was used as an internal control. *Irp9* and *aroG* expression levels were normalized to 1 in line nahG-catA-1.2 × irp9-aroG 4.9 and were calculated relative to these values in the other lines. Error bars represent the SD from technical duplicates. (**D**) MA content in mature senesced dried stems of nahG-catA-1.2 and nahG-catA-1.2 × irp9-aroG transgenic lines. Error bars represent the SE from four biological replicates ($n = 4$). Asterisks indicate significant differences from the nahG-catA-1.2 line using the unpaired Student's *t*-test (*$P < 0.001$).

stems of homozygous plants at the T3 generation (Fig. 3C). For these six lines, the content of SA extracted from 15-cm stems was increased significantly 11- to 65-fold compared to wild-type plants (Fig. 3D). The two lines showing the highest SA increase (irp9-aroG-1.3 and irp9-aroG-3.11) had an obvious dwarf phenotype compared to the other lines and wild-type plants (data not shown), a phenomenon previously observed in Arabidopsis mutants that overproduce SA (Sha, 2003). Therefore, co-expression of Irp9 and AroG* genes under secondary cell wall promoters represents an efficient strategy for over-producing SA in Arabidopsis stems.

3.3. MA production in plants expressing NahG, CatA, Irp9, and AroG*

To assess the effect of SA over-accumulation on MA production, the line nahG-catA-1.2 was transformed with the constructs used for expression of *irp9* and for co-expression of *irp9* and *aroG**(Fig. 1B). First, we selected several transgenic lines that show expression of *irp9* in the nahG-catA-1.2 background (Fig. 4A). Muconic acid content in stems of senesced nahG-catA-1.2 × irp9 lines was increased 2- to 24-fold compared to the parental line (Fig. 4B). Second, several transgenic lines that show co-expression of *irp9* and *aroG** in the nahG-catA-1.2 genetic background were selected (Fig. 4C). In these lines, muconic acid content range between 483 and 637 µg/g DW, which represents a 39- to 51-fold increase compared to the values measured in the nahG-catA-1.2 parental line (Fig. 4D). These results demonstrate the positive effect of increasing the carbon flux through the SA route to enhance the production of MA in the proposed biosynthetic pathway. Furthermore, measurement of SA and catechol in two MA-producing lines revealed contents far below those of MA, suggesting that these two intermediates could limit MA biosynthesis (Supplementary Fig. S2).

4. Discussion and conclusions

We demonstrate in this work that bacterial catechol 1,2-dioxygenase (CatA) is functional in Arabidopsis plastids and thus can be exploited for the production of MA in plants. A biosynthetic route for catechol has been elegantly demonstrated in white campion flowers: it originates from phenylalanine and uses cinnamic acid, benzoic acid, and SA as intermediates (Akhtar and Pichersky, 2013). In this pathway, the biosynthetic genes involved in the steps for sequential conversion of benzoic acid into SA and catechol remain to be identified. Therefore, a plastid-targeted bacterial salicylate hydroxylase (NahG) was used in this work for the conversion of chorismate-derived SA into catechol. Gratifyingly, co-expression of NahG and CatA in plastids resulted in the

production of MA, and MA titers could be further enhanced by increasing the carbon flux through SA biosynthetic pathway. Although the synthesis of SA from chorismate involves known plastidial isochorismate synthases, the plant enzyme(s) involved in the conversion of isochorismate into SA remain to be identified (Widhalm and Dudareva, 2015). Similarly, the identity and sub-cellular localization(s) of the enzymes that contribute to SA biosynthesis from cinnamic acid — an alternative SA pathway described in several plant species — have not all been elucidated (Dempsey et al., 2011). Therefore, we targeted to plastids a characterized bacterial bi-functional SA synthase (isochorismate synthase / isochorismate pyruvate lyase, Irp9) that has been previously validated *in planta* to enhance SA synthesis in Arabidopsis. Moreover, expression of plastid-targeted bacterial feedback-insensitive AroG enhanced SA production when co-expressed with Irp9, which confirms previous observations in Arabidopsis about the positive effect of AroG expression on the accumulation of metabolites derived from the shikimate pathway (Tzin et al., 2012). Considering low SA titers measured in our transgenic Arabidopsis lines that produce MA (Supplementary Fig. S2), additional engineering to enhance carbon flux through SA in these lines could improve MA titers. Whether the overexpression of other enzymes from the shikimate pathway (Fig. 1A, steps 2–7) would further increase the SA pool remains to be investigated. Similarly, the enolase responsible for the synthesis of phosphoenolpyruvate (Fig. 1A, step 1) could be targeted to increase SA content via the shikimate pathway since its overexpression was shown to drive carbon flux towards aromatic amino acid biosynthesis in tomato (Zhang et al., 2015). Specifically, the lack of correlation observed between aroG expression levels and SA (Fig. 3C-D) or MA (Fig. 4C-D) titers in our engineered plants suggests that one of the two aroG substrates could become limiting (Fig. 1A). Ultimately, since our MA biosynthetic route is confined to plastids, a trapping of SA inside plastids should be considered to avoid leak of this precursor, which could be achieved by downregulating known SA plastid exporters (Serrano et al., 2013).

More generally, certain crops engineered for reduced biomass recalcitrance and enhanced digestibility overproduce SA (Gallego-Giraldo et al., 2011), making them ideal genetic backgrounds for the production of both fermentable sugars and value-added MA. Likewise, bioenergy *Populus* species (e.g., Salicaceae family) known to accumulate extremely high amounts of endogenous SA and SA-derived metabolites (up to 10% leaf dry weight) would represent adequate plant chassis for MA bioproduction (Lindroth and Hwang, 1996; Morse et al., 2007). In addition, we anticipate that bioenergy crops engineered for MA accumulation could serve as compatible feedstock for MA-producing microbial strains able to grow on lignin-enriched streams derived from lignocellulosic biomass (Vardon et al., 2015; Rodriguez et al., 2017). Because such streams are generated with high solids loadings (> 10% w/v), their enrichment with MA could be achieved using biomass containing MA. As an illustration, biomass containing 5% MA DW could potentially generate streams with 5 g/L MA (at 10% w/v biomass loading), a value similar to the best titers accomplished using engineered microbes and glucose as carbon source (Johnson et al., 2016). In this scenario, the MA titer we are reporting in Arabidopsis (0.64 mg/g DW) would need to be improved by less than two orders of magnitude. More research will be needed to determine the optimal biomass pretreatment conditions for the release of MA. Our preliminary study indicates that optimal dilute alkaline biomass pretreatments used to generate lignin-rich fractions for downstream biological upgrading (Karp et al., 2014) can efficiently release MA from biomass of our engineered Arabidopsis plants (Supplementary Fig. S3). On the other hand, lower amount of MA was recovered when biomass was treated with dilute acid, possibly due to the cyclization of MA into muconolactone under these conditions (Carraher et al., 2017).

As complementary approaches to the strategy presented in this work, the synthesis of catechol towards MA production could be achieved from alternate precursors such as anthranilate, protocatechuate, or 4-hydroxybenzoate as previously achieved in microorganisms (Kruyer and Peralta-Yahya, 2017). For this purpose, our preliminary work conducted in tobacco validated that both anthranilate 1,2-dioxygenase and protocatechuate decarboxylase can be functionally expressed in plastids for the synthesis of catechol from anthranilate and protocatechuate, respectively (Shih et al., 2016a). In addition, previous engineering strategies in Arabidopsis have demonstrated the overproduction of anthranilate, protocatechuate, and 4-hydroxybenzoate from chorismate (Eudes et al., 2016; Ishihara et al., 2006; Last and Fink, 1988). Since protocatechuate and 4-hydroxybenzoate synthesis can also be accomplished from the precursors 3-dehydroshikimate and *p*-coumaroyl-CoA, respectively (Eudes et al., 2012, 2016; Wu et al., 2017), production of high MA titers in plants could be envisioned by stacking branched biosynthetic routes that use diverse intermediates and products of the shikimate pathway (Supplementary Fig. S4), and assisted by the use of synthetic promoters to optimize and synchronize the expression of multiple biosynthetic genes (Shih et al., 2016b).

Acknowledgements

This work was part of the DOE Joint BioEnergy Institute (http://www.jbei.org) supported by the U. S. Department of Energy, Office of Science, Office of Biological and Environmental Research, through contract DE-AC02-05CH11231 between Lawrence Berkeley National Laboratory and the U.S. Department of Energy. The United States Government retains and the publisher, by accepting the article for publication, acknowledges that the United States Government retains a non-exclusive, paid-up, irrevocable, world-wide license to publish or reproduce the published form of this manuscript, or allow others to do so, for United States Government purposes.

Competing interests

DL has financial conflicts of interest in Afingen Inc. and Bayer CropScience.

Appendix A. Supporting information

Supplementary data associated with this article can be found in the online version at http://dx.doi.org/10.1016/j.ymben.2018.02.002.

References

Akhtar, T.A., Pichersky, E., 2013. Veratrole biosynthesis in white campion. Plant Physiol. 162, 52–62.

Barton, N., Horbal, L., Starck, S., Kohlstedt, M., Luzhetskyy, A., Wittmann, C., 2017. Enabling the valorization of guaiacol-based lignin: integrated chemical and biochemical production of cis,cis-muconic acid using metabolically engineered *Amycolatopsis* sp ATCC 39116. Metab. Eng. http://dx.doi.org/10.1016/j.ymben.2017.12.001.

Bechtold, N., Pelletier, G., 1998. In planta Agrobacterium-mediated transformation of adult Arabidopsis thaliana plants by vacuum infiltration. Methods Mol. Biol. 82, 259–266.

Bell-Lelong, D.A., Cusumano, J.C., Meyer, K., Chapple, C., 1997. Cinnamate-4-hydroxylase expression in Arabidopsis. Regulation in response to development and the environment. Plant Physiol. 113, 729–738.

Börnke, F., Broer, I., 2010. Tailoring plant metabolism for the production of novel polymers and platform chemicals. Curr. Opin. Plant Biol. 13, 354–362.

Carraher, J.M., Pfennig, T., Rao, R.G., Shanks, B.H., Tessonnier, J.-P., 2017. Cis,cis-Muconic acid isomerization and catalytic conversion to biobased cyclic-C_6-1,4-diacid monomers. Green Chem. 19, 3042–3050.

Dempsey, D.A., Vlot, A.C., Wildermuth, M.C., Klessig, D.F., 2011. Salicylic acid biosynthesis and metabolism. Arabidopsis Book 9, e0156.

Do, C.T., Pollet, B., Thévenin, J., Sibout, R., Denoue, D., Barrière, Y., Lapierre, C., Jouanin, L., 2007. Both caffeoyl Coenzyme A 3-O-methyltransferase 1 and caffeic acid O-methyltransferase 1 are involved in redundant functions for lignin, flavonoids and sinapoyl malate biosynthesis in Arabidopsis. Planta 226, 1117–1129.

Eudes, A., George, A., Mukerjee, P., Kim, J.S., Pollet, B., Benke, P.I., Yang, F., Mitra, P., Sun, L., Cetinkol, O.P., Chabout, S., Mouille, G., Soubigou-Taconnat, L., Balzergue, S., Singh, S., Holmes, B.M., Mukhopadhyay, A., Keasling, J.D., Simmons, B.A., Lapierre, C., Ralph, J., Loqué, D., 2012. Biosynthesis and incorporation of side-chain-truncated lignin monomers to reduce lignin polymerization and enhance saccharification. Plant

Biotechnol. J. 10, 609–620.
Eudes, A., Sathitsuksanoh, N., Baidoo, E.E., George, A., Liang, Y., Yang, F., Singh, S., Keasling, J.D., Simmons, B.A., Loqué, D., 2015. Expression of a bacterial 3-dehydroshikimate dehydratase reduces lignin content and improves biomass saccharification efficiency. Plant Biotechnol. J. 13, 1241–1250.
Eudes, A., Pereira, J.H., Yogiswara, S., Wang, G., Teixeira Benites, V., Baidoo, E.E., Lee, T.S., Adams, P.D., Keasling, J.D., Loqué, D., 2016. Exploiting the substrate promiscuity of hydroxycinnamoyl-CoA: shikimate hydroxycinnamoyl transferase to reduce lignin. Plant Cell Physiol. 57, 568–579.
Farré, G., Blancquaert, D., Capell, T., Van Der Straeten, D., Christou, P., Zhu, C., 2014. Engineering complex metabolic pathways in plants. Annu. Rev. Plant Biol. 65, 187–223.
Friedrich, L., Vernooij, B., Gaffney, T., Morse, A., Ryals, J., 1995. Characterization of tobacco plants expressing a bacterial salicylate hydroxylase gene. Plant Mol. Biol. 29, 959–968.
Gallego-Giraldo, L., Escamilla-Trevino, L., Jackson, L.A., Dixon, R.A., 2011. Salicylic acid mediates the reduced growth of lignin down-regulated plants. Proc. Natl. Acad. Sci. U S A. 108, 20814–20819.
Haushalter, R.W., Phelan, R.M., Hoh, K.M., Su, C., Wang, G., Baidoo, E.E., Keasling, J.D., 2017. Production of odd-carbon dicarboxylic acids in *Escherichia coli* using an engineered biotin-fatty acid biosynthetic pathway. J. Am. Chem. Soc. 139, 4615–4618.
Ishihara, A., Asada, Y., Takahashi, Y., Yabe, N., Komeda, Y., Nishioka, T., Miyagawa, H., Wakasa, K., 2006. Metabolic changes in *Arabidopsis thaliana* expressing the feedback-resistant anthranilate synthase alpha subunit gene OASA1D. Phytochemistry 67, 2349–2362.
Johnson, C.W., Salvachúa, D., Khanna, P., Smith, H., Peterson, D.J., Beckham, G.T., 2016. Enhancing muconic acid production from glucose and lignin-derived aromatic compounds via increased protocatechuate decarboxylase activity. Metab. Eng. Commun. 3, 111–119.
Johnson, C.W., Abraham, P.E., Linger, J.G., Khanna, P., Hettich, R.L., Beckham, G.T., 2017. Eliminating a global regulator of carbon catabolite repression enhances the conversion of aromatic lignin monomers to muconate in *Pseudomonas putida* KT2440. Metab. Eng. Commun. 5, 19–25.
Karp, E.M., Donohoe, B.S., O'Brien, M.H., Ciesielski, P.N., Mittal, A., Biddy, M.J., Beckham, G.T., 2014. Alkaline pretreatment of corn stover: bench-scale fractionation and stream characterization. ACS Sustain. Chem. Eng. 2, 1481–1491.
Kruyer, N.S., Peralta-Yahya, P., 2017. Metabolic engineering strategies to bio-adipic acid production. Curr. Opin. Biotechnol. 45, 136–143.
Last, R.L., Fink, G.R., 1988. Tryptophan-requiring mutants of the plant *Arabidopsis thaliana*. Science 240, 305–310.
Lebrun, M., Leroux, B., Sailland, A., 1992. Gène chimère pour la transformation des plantes. European patent application. Patent Application No. EP 508909A1.
Lindroth, R.L., Hwang, S.Y., 1996. Diversity, redundancy and multiplicity in chemical defense systems of aspen. Recent Adv. Phytochem. 30, 25–56.
Livak, K.J., Schmittgen, T.D., 2011. Analysis of relative gene expression data using real-time quantitative PCR and the 2(-Delta Delta C(T)) method. Methods 25, 402–408.
Maeda, H., Dudareva, N., 2012. The shikimate pathway and aromatic amino acid biosynthesis in plants. Annu. Rev. Plant Biol. 63, 73–105.
Matthiesen, J.E., Carraher, J.M., Vasiliu, M., Dixon, D.A., Tessonnier, J.-P., 2016. Electrochemical conversion of muconic acid to biobased diacid monomers. ACS Sustain. Chem. Eng. 4, 3575–3585.
Morse, A.M., Tschaplinski, T.J., Dervinis, C., Pijut, P.M., Schmelz, E.A., Day, W., Davis, J.M., 2007. Salicylate and catechol levels are maintained in nahG transgenic poplar. Phytochemistry 68, 2043–2052.
Persson, S., Caffall, K.H., Freshour, G., Hilley, M.T., Bauer, S., Poindexter, P., Hahn, M.G., Mohnen, D., Somerville, C., 2007. The *Arabidopsis irregularxylem8* mutant is deficient in glucuronoxylan and homogalacturonan, which are essential for secondary cell wall integrity. Plant Cell. 19, 237–255.
Rodriguez, A., Salvachua, D., Katahira, R., Black, B.A., Cleveland, N.S., Reed, M., Smith, H., Baidoo, E.E.K., Keasling, J.D., Simmons, B.A., Beckham, G.T., Gladden, J.M., 2017. Base-catalyzed depolymerization of solid lignin-rich streams enables microbial conversion. ACS Sustain. Chem. Eng. 5, 8171–8180.
Serrano, M., Wang, B., Aryal, B., Garcion, C., Abou-Mansour, E., Heck, S., Geisler, M., Mauch, F., Nawrath, C., Métraux, J.P., 2013. Export of salicylic acid from the chloroplast requires the multidrug and toxin extrusion-like transporter EDS5. Plant Physiol. 162, 1815–1821.
Sha, J., 2003. The salicylic acid loop in plant defense. Curr. Opin. Plant Biol. 6, 365–371.
Shih, P.M., Vuu, K., Eudes, A., Loqué D., 2016a. Bioproduction of muconic acid in plants. International Conference on Plant Synthetic Biology and Bioengineering, Miami Beach, FL. Dec. 16–18.
Shih, P.M., Liang, Y., Loqué, D., 2016b. Biotechnology and synthetic biology approaches for metabolic engineering of bioenergy crops. Plant J. 87, 103–117.
Snell, K.D., Singh, V., Brumbley, S.M., 2015. Production of novel biopolymers in plants: recent technological advances and future prospects. Curr. Opin. Biotechnol. 32, 68–75.
Sonoki, T., Morooka, M., Sakamoto, K., Otsuka, Y., Nakamura, M., Jellison, J., Goodell, B., 2014. Enhancement of protocatechuate decarboxylase activity for the effective production of muconate from lignin-related aromatic compounds. J. Biotechnol. 192 (Pt A), 71–77.
Sonoki, T., Takahashi, K., Sugita, H., Hatamura, M., Azuma, Y., Sato, T., Suzuki, S., Kamimura, N., Masai, E., 2017. Glucose-free cis,cis-muconic acid production via new metabolic designs corresponding to the heterogeneity of lignin. ACS Sustain. Chem. Eng. http://dx.doi.org/10.1021/acssuschemeng.7b03597.
Tzin, V., Malitsky, S., Ben Zvi, M.M., Bedair, M., Sumner, L., Aharoni, A., Galili, G., 2012. Expression of a bacterial feedback-insensitive 3-deoxy-D-arabino-heptulosonate 7-phosphate synthase of the shikimate pathway in Arabidopsis elucidates potential metabolic bottlenecks between primary and secondary metabolism. New Phytol. 194, 430–439.
Vaillancourt, F.H., Bolin, J.T., Eltis, L.D., 2006. The ins and outs of ring-cleaving dioxygenases. Crit. Rev. Biochem. Mol. Biol. 41, 241–267.
Vardon, D.R., Franden, M.A., Johnson, C.W., Karp, E.M., Guarnieri, M.T., Linger, J.G., Salm, M.J., Strathmann, T.J., Beckham, G.T., 2015. Adipic acid production from lignin. Energy Environ. Sci. 8, 617–628.
Vega-Sánchez, M.E., Loqué, D., Lao, J., Catena, M., Verhertbruggen, Y., Herter, T., Yang, F., Harholt, J., Eb,ert, B., Baidoo, E.E., Keasling, J.D., Scheller, H.V., Heazlewood, J.L., Ronald, P.C., 2015. Engineering temporal accumulation of a low recalcitrancepolysaccharide leads to increased C6 sugar content in plant cell walls. Plant Biotechnol. J. 13, 903–914.
Widhalm, J.R., Dudareva, N., 2015. A familiar ring to it: biosynthesis of plant benzoic acids. Mol. Plant 8, 83–97.
Wu, W., Dutta, T., Varman, A., Eudes, A., Manalansan, B., Loqué, D., Singh, S., 2017. Lignin valorization: two hybrid biochemical routes for the conversion of polymeric lignin into value-added chemicals. Sci. Rep. 7, 8420.
Xie, N.Z., Liang, H., Huang, R.B., Xu, P., 2014. Biotechnological production of muconic acid: current status and future prospects. Biotechnol. Adv. 32, 615–622.
Xue, L.J., Guo, W., Yuan, Y., Anino, E.O., Nyamdari, B., Wilson, M.C., Frost, C.J., Chen, H.Y., Babst, B.A., Harding, S.A., Tsai, C.J., 2013. Constitutively elevated salicylic acid levels alter photosynthesis and oxidative state but not growth in transgenic *Populus*. Plant Cell 25, 2714–2730.
Yang, F., Mitra, P., Zhang, L., Prak, L., Verhertbruggen, Y., Kim, J.S., Sun, L., Zheng, K., Tang, K., Auer, M., Scheller, H.V., Loqué, D., 2013. Engineering secondary cell wall deposition in plants. Plant Biotechnol. J. 11, 325–335.
Yuan, L., Grotewold, E., 2015. Metabolic engineering to enhance the value of plants as green factories. Metab. Eng. 27, 83–91.
Zhang, Y., Butelli, E., Alseekh, S., Tohge, T., Rallapalli, G., Luo, J., Kawar, P.G., Hill, L., Santino, A., Fernie, A.R., Martin, C., 2015. Multi-level engineering facilitates the production of phenylpropanoid compounds in tomato. Nat. Commun. 6, 8635.